Lead Isotope Geochemistry of Paleoproterozoic Layered Intrusions in the Eastern Baltic Shield: Inferences About Magma Sources and U-Th-Pb Fractionation in the Crust-Mantle System

Article *in* Geochimica et Cosmochimica Acta · February 1998

DOI: 10.1016/S0016-7037(98)00056-8

CITATIONS
14

READS
45

2 authors:

Yuri Amelin
Australian National University
246 PUBLICATIONS **8,264** CITATIONS

SEE PROFILE

Leonid A. Neymark
United States Geological Survey
155 PUBLICATIONS **1,710** CITATIONS

SEE PROFILE

Pergamon

Geochimica et Cosmochimica Acta, Vol. 62, No. 3, pp. 493–505, 1998

0016-7037/98 $19.00 + .00

PII S0016-7037(98)00056-8

Lead isotope geochemistry of Paleoproterozoic layered intrusions in the eastern Baltic Shield: Inferences about magma sources and U-Th-Pb fractionation in the crust-mantle system

YURI V. AMELIN[1] and LEONID A. NEYMARK[2,*]

[1]Jack Satterly Geochronology Laboratory, Royal Ontario Museum, Toronto, Ontario M5S 2C6, Canada
[2]Institute of Precambrian Geology and Geochronology, Russian Academy of Science, St. Petersburg 199034, Russia

(*Received June* 13, 1996; *accepted in revised form October* 2, 1997)

Abstract—U-Pb data for plagioclase and sulfide are reported from the Burakovka and Olanga layered mafic-ultramafic complexes in Karelia. These 2.44–2.45 Ga complexes differ in the age of their host rocks and in post-emplacement metamorphic history. Acid leaching of optically discrete plagioclase populations revealed three components of Pb present in the Olanga plagioclases: initial, radiogenic, and alteration-related. Leaching in HCl and HNO_3 was found to remove most of U and radiogenic Pb from plagioclase and to fractionate U from Pb. The alteration component, abundant in the Olanga plagioclase, is only partially removed by leaching. The Olanga sulfides also contain a significant radiogenic component. Plagioclase from the unmetamorphosed Burakovka Complex yields more reliable initial Pb ratios.

The Pb isotopic compositions of plagioclase from the three intrusions of the Olanga Complex form a single steep linear trend, which shows excess scatter due to residual radiogenic and alteration Pb. Calculated single-stage μ_1* of about 7.9 in the Kivakka intrusion is close to the Archean depleted mantle value, but combined Pb, Sr, and Nd isotopic systematics suggest the presence of an enriched component from either lithospheric or slightly contaminated plume source. Internal variations in initial Pb and Sr isotopic ratios and Pb isotopic systematics of sulfides are explained by late-magmatic fluid exchange with 2.7 Ga country rocks.

The Burakovka Complex, emplaced into the pre-3.1 Ga crust, shows large correlated variations in $^{207}Pb/^{204}Pb$, $\epsilon_{Nd}(T)$ and $^{87}Sr/^{86}Sr(T)$ in plagioclase. Initial Pb, Nd, and Sr isotopic variations in the Burakovka Complex are interpreted as a result of a multistage contamination process, including contamination en route and during emplacement and local assimilation of enclosing gneiss. In addition, the Burakovka mantle source was probably modified with addition of sediment-derived Pb by a subduction-zone fluid.

Time-integrated Th/U $\approx$ 4.3 in mantle sources and crustal contaminants of the Olanga and Burakovka complexes are uniform and are similar to the Archean mantle value. This implies that U/Pb fractionation in the Archean-Paleoproterozoic crust-mantle system probably occurred by hydrothermal Pb transfer that fractionated Pb from U, but not Th from U. *Copyright © 1998 Elsevier Science Ltd*

1. INTRODUCTION

Variations of initial Pb isotopic compositions in ancient rocks provide a powerful tool for understanding the early evolution of the crust-mantle system. The initial Pb isotopic composition usually cannot be accurately determined by measuring Pb isotopic ratios in a rock and applying correction for radiogenic growth. Two alternative ways are used to assess the Pb isotopic signatures in sources of ancient igneous rocks: (1) study of cogenetic series of whole rock samples and (2) analysis of minerals of known age, having low U/Pb and Th/Pb ratios. The first approach is similar to Sm-Nd and Rb-Sr whole rock isochron dating methods and allows one to determine simultaneously a crystallization age and an average single-stage model $^{238}U/^{204}Pb$ (μ_1*) in the sources of magmas (e.g., Dupré and Arndt, 1990). The limitations are also similar for the Pb-Pb, Rb-Sr, and Sm-Nd whole-rock methods: an interpretation relies on considering a linear array as an isochron, which may be difficult to recognize from a mixing line or a trend generated by metamorphic or hydrothermal alteration. Initial isotopic heterogeneity or variable contamination results in scattered arrays, for which precise interpretation is impossible, or in isochrons with initial slope, yielding biased age and initial μ value.

A study of Pb isotopic composition in low-U/Pb, Th/Pb minerals is free of assumptions involved in whole rock isochron approach and allows a direct evaluation of source heterogeneity and mixing processes. The principal limitation here is the difficulty of determining the true initial Pb isotopic composition at the time of crystallization, because open-system behavior during post-magmatic processes and/or regional metamorphism impart Pb isotopic heterogeneity in minerals commonly used for this purpose: K-feldspar (Ludwig and Silver, 1977; Gariépy and Allègre, 1985; McNaughton and Bickle, 1987; Housh and Bowring, 1991) and sulfides (e.g., Brévart et al., 1986; Dupré and Arndt, 1990). Determination of initial Pb in ancient mafic-ultramafic rocks is particularly difficult, because K-feldspar is usually absent, and plagioclase, another potentially useful mineral, has low Pb concentrations and often higher U/Pb than K-feldspar (Oversby, 1975; Leeman, 1979; Waters et al., 1990). In addition, correct interpretation of initial Pb data relies on precise crystallization age determination.

A suite of mafic layered intrusions, emplaced into the Archean province of the Baltic Shield at the beginning of the Proterozoic, provides an efficient probe for the crust-mantle system formed by the end of the Archean. The intrusions were

* Author to whom correspondence should be addressed (lneymark@usgs.gov).

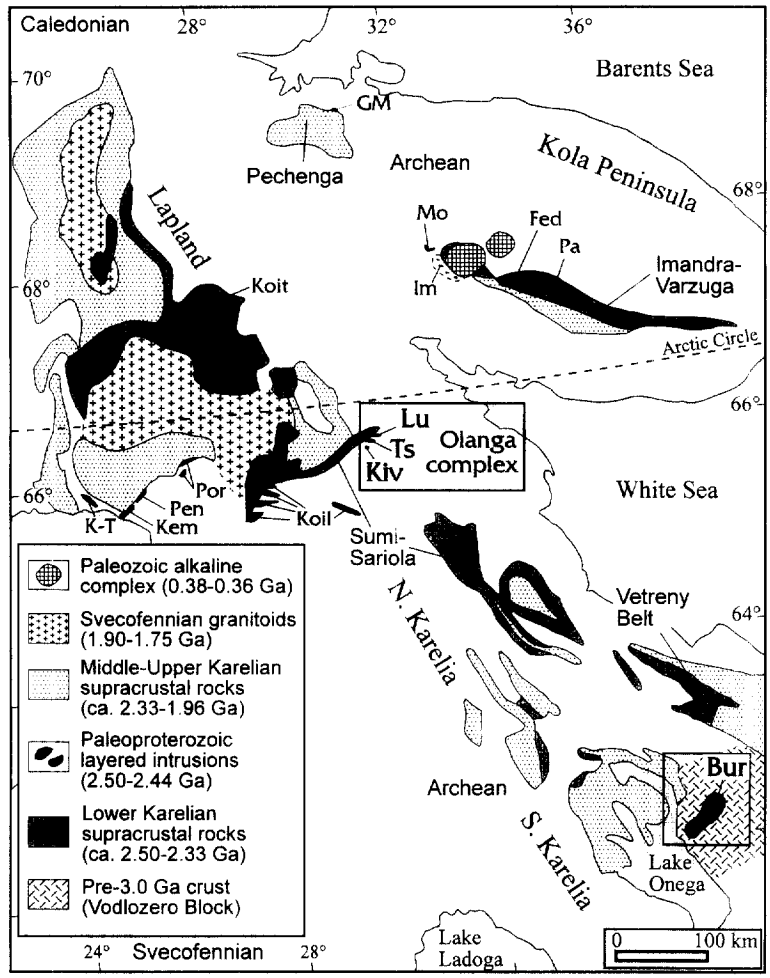

Fig. 1. Geological sketch map of the eastern Baltic Shield, showing distribution of Paleoproterozoic rocks and location of studied plutons (modified from Gorbunov et al., 1985 and Alapieti et al., 1990). Layered intrusions studied in this work: Bur-Burakovka, Kiv-Kivakka, Lu-Lukkulaisvaara, Ts-Tsipringa. Other layered intrusions: Fed-Fedorova Tundra, GM-General'skaya Mountain, Im-Imandra lopolith, Kem-Kemi, Koil-Koillismaa Complex, Koit-Koitelainen, K-T-Kukkola-Tornio, Mo-Monche pluton, Pa-Pana Tundra, Pen-Penikat, Por-Portimo Complex.

emplaced into the crust with different age and evolution histories and were variably affected by a regional metamorphism in the middle Proterozoic. The objectives of this study are: (1) to determine the initial Pb isotopic compositions in plagioclase from variably metamorphosed mafic igneous rocks, (2) to evaluate a possible connection between the Pb isotopic characteristics of continental mafic magmatism and the crustal basement age, and (3) to infer possible implications for the U-Th-Pb fractionation in the Archean crust-mantle system.

2. GEOLOGICAL FRAMEWORK AND PREVIOUS ISOTOPIC STUDIES

The 2.50–2.44 Ga Sumi-Sariola igneous province of the eastern Baltic Shield (Fig. 1) is composed of layered mafic intrusions and dikes, mafic, and felsic volcanics and granitoids and is thought to be formed during early stages of continental rifting. Recent compilations of geology and geochronology of the Sumi-Sariola rocks and detailed geological and petrologic data for the layered intrusions are presented by Alapieti et al. (1990), Turchenko (1992), Semenov et al. (1994, 1995), Amelin et al. (1995), Amelin and Semenov (1996), and Puchtel et al. (1996, 1997). The disseminated Ni-Cu sulfide mineralization associated with the layered intrusions is described by Turchenko et al. (1991) and Turchenko (1992). Layered intrusions studied in this work include three intrusions of the Olanga Complex, northern Karelia: Kivakka (2445 Ma), Tsipringa (2441 Ma), and Lukkulaisvaara (2442 Ma), and the 2449 Ma Burakovka Complex, southeastern Karelia.

Layered intrusions and volcanics of the Sumi-Sariola are located within Archean granite-gneisses. The plagiogneisses and granitoids of northern Karelia, which enclose the Olanga Complex, have U-Pb zircon ages of 2.70 Ga (Buiko et al., 1994) and Sm-Nd depleted mantle model ages of 2.77–2.79 Ga (Amelin and Turchenko, unpubl. data). The basement rocks of the Olanga Complex thus comprise a juvenile late Archean crust without significant involvement of a much older crust. Regional greenschist facies metamorphism in northern Karelia

was dated at 1755 ± 27 Ma by concordant U-Pb titanite and apatite ages from the Lukkulaisvaara and Tsipringa intrusions (Amelin et al., 1995). K-Ar ages of amphibole, biotite, and muscovite from the Sumi-Sariola basalt and rhyolite are 1680–1490 Ma (Buiko et al., 1994).

The Vodlozero block of southeastern Karelia, which hosts the Burakovka Complex, is made up of substantially older rocks and possibly contains the oldest rocks in the Baltic Shield. The crystallization ages of protholiths of the Vodlozero gneisses and amphibolites are not well established, but can be as old as 3.15–3.55 Ga, as indicated by Sm-Nd model ages (Lobach-Zhuchenko et al., 1993). The Vodlozero block underwent at least two stages of metamorphism and deformation at 3.13–3.21 Ga and 2.82–2.86 Ga (U-Pb zircon, Lobach-Zhuchenko et al., 1993). The latest low-grade metamorphic episode in the Vodlozero block is indicated by a 2480–2540 Ma by the U-Pb apatite age from the gneiss and the Kubovo late-kinematic granite (Sergeev et al., 1990; Ovchinnikova et al., 1991).

3. SAMPLES AND ANALYTICAL PROCEDURES

The samples analyzed in this study are gabbronorites and norites, including olivine-bearing varieties, and were collected from outcrop (Olanga and Burakovka complexes) and a drill core (Burakovka Complex). Plagioclase, An_{55} to An_{80}, is the most abundant cumulus mineral in these samples, composing 40–70% of rock volume. The Olanga sulfides analyzed in this study are pyrrhotite and chalcopyrite from pyroxenite, norite, and gabbronorite.

Plagioclase and sulfide fractions were separated at the Institute of Precambrian Geology and Geochronology (IPGG) using magnetic and heavy liquid techniques. Pb isotopic analyses of sulfide separates were performed at the IPGG, following the procedure described by Neymark et al. (1994). Pb isotope ratios were measured on a MAT-261 multicollector mass-spectrometer in static mode and corrected for mass-discrimination of 0.0013 ± 0.0003 amu^{-1}, as determined by replicate analyses of NIST standard SRM 982, using standard values of Todt et al. (1993). Procedure blank was 5 ± 2 ng Pb.

All U-Pb analyses of plagioclase and sulfide separates were completed at the Royal Ontario Museum (ROM). Optically homogeneous fractions were handpicked in ethanol under a binocular microscope and examined at high magnification on white and black backgrounds. The plagioclase fractions were subsequently leached in warm 6N HCl and in 7N HNO_3 (30 min in each acid). Sulfides were washed in 6N HCl only. Before leaching, and after each leaching step, the fractions were rinsed with ultrapure water and distilled acetone, dried, and weighed on a microbalance with resolution 10^{-6} g. The difference in weights before and after leaching was taken as a leachate weight (Table 1). For the Olanga samples, the leachates were combined, and for the Burakovka samples, the HCl and HNO_3 leachates were analyzed separately. The leaching procedure was identical for all plagioclase fractions, but leachates were analyzed only from selected fractions.

Both residues and leachates were spiked with mixed ^{235}U-^{205}Pb tracer. Some fractions were also spiked with mixed ^{85}Rb-^{84}Sr and ^{149}Sm-^{150}Nd tracers. Plagioclase residues were dissolved in HF-HNO_3 in 3 mL PFA teflon vials. Sulfides were dissolved in 7N HNO_3. U and Pb were separated using HCl-HBr-HNO_3 anion exchange procedures and loaded together on Re single filaments with silica gel emitter. Pb from most plagioclase residues was analyzed using a single Faraday collector on a VG-354 mass spectrometer. Some fractions were measured in static multicollector mode on another VG-354 mass spectrometer, calibrated for collector efficiencies using a stable ion beam. Multiple analyses of the SRM-981 standard revealed no systematic differences between single collector and static multicollector results. All U fractions and Pb from most leachates and two residues were analyzed using Daly photomultiplier. Procedure blanks were 5.0 ± 1.5 pg for Pb and 0.25 ± 0.10 pg for U (2 s.d.). Average isotopic composition of Pb blank was $^{207}Pb/^{206}Pb$ = 0.853 ± 0.005, $^{208}Pb/^{206}Pb$ = 2.061 ± 0.014, and $^{206}Pb/^{204}Pb$ = 17.9 ± 0.6 (2 s.d.). Blank corrections, with magnification of errors to account for blank uncertainties, were applied to U and Pb concentrations, U/Pb ratios, and Pb isotopic compositions. Fractionation correction was 0.0010 ± 0.0004 amu^{-1} for Pb in both single collector and static multicollector modes, and 0.0013 ± 0.0003 amu^{-1} for U, based on replicate analyses of SRM 981 (using standard values of Todt et al., 1993) and SRM U-500 standards, respectively. Regression lines were calculated using the ISOPLOT program (Ludwig, 1992), the parameters are reported at 95% confidence level. Errors of the mean values are given as 2 standard deviations.

Rb, Sr, Sm, and Nd were separated from washes of anion-exchange columns and analyzed using the procedure described by Amelin at al. (1997). Procedure blanks are 1.5 ± 0.5 pg Rb, 30 ± 12 pg Sr and <5 pg Sm and Nd.

4. RESULTS

4.1. Leaching Experiments

The U-Pb data for acid leachates and residues are presented in Tables 1 and 2. In the Kivakka and Tsipringa C-110 plagioclases, where 12–43% of the total fractions were dissolved in HCl and HNO_3, Pb concentrations in leachates and residues are nearly identical. In the other Tsipringa and in the Burakovka samples, where only a small part (0.8–5%) of the plagioclase was dissolved, Pb concentrations in leachates vary considerably and can be either higher or lower than in the residues. Uranium concentrations in leachates of all samples, except KV-570 (# 7, Table 1), are much higher than in residues. The U-Pb isotopic systematics of the leachates and residues are shown in Fig. 2 (data for fraction 12 are not plotted, because U amount in the leachate is extremely small (0.3 pg) and U/Pb ratio is, therefore, imprecise). Variations of $^{238}U/^{204}Pb$ (μ) and $^{206}Pb/^{204}Pb$ between leachates and residues are much smaller in the Olanga than in the Burakovka samples. The Pb isotopic composition in the leachates is more radiogenic than in the residues in all fractions, except KV-570, where it is identical within error. Progressive leaching of the Burakovka samples shows that three of four studied fractions (# 44, 46, and 48, Table 2) contain unsupported radiogenic Pb, which is preferentially leached during the first (HCl) step. Subsequent HNO_3 treatment removes both a U-bearing component and the residual radiogenic Pb. The fourth Burakovka fraction (# 43) demonstrates behavior consistent with progressive dissolution of a U-bearing phase without substantial fractionation of U and Pb. The apparent age of U-Pb leachate-residue "isochron" for fraction 43 (Fig. 2b) is ca. 2340 Ma and is close to the crystallization age.

Pb isotopic compositions in leachates and residues of the Olanga plagioclases (Fig. 3a) are very similar, and no estimates of leachate-residue "isochro" ages are possible because $^{207}Pb/^{204}Pb$ in all pairs are similar within the 2σ error limits. A much greater range in Pb isotopic composition is observed in the Burakovka plagioclase leachates (Fig. 3b), all of which contain more radiogenic Pb than the residues. All seven leachates of four Burakovka plagioclases define a $^{207}Pb/^{204}Pb$-$^{206}Pb/^{204}Pb$ isochron with MSWD = 1.7, the slope of which corresponds to an age of 2309 ± 350 Ma, within error of the crystallization age. Elevated $^{208}Pb/^{204}Pb$ in plagioclase leachates compared to residues in both Olanga and Burakovka complexes (Fig. 3c) indicates that radiogenic ^{208}Pb is also more easily extracted by the acids than initial common Pb.

Table 1. U-Pb data for plagioclase and sulfide fractions from the Olanga Complex

Fraction number	Sample	Fraction description	Leaching	Fraction wt, mg	U ppm	Pb ppm	$^{238}U/^{204}Pb$	$^{206}Pb/^{204}Pb$	$^{207}Pb/^{204}Pb$	$^{208}Pb/^{204}Pb$	μ_1*	κ*
Kivakka intrusion												
1	KV-401	col clear + w tur	R	1.535	0.0073	1.234	0.3232±54	13.828± 22	14.712± 26	33.759± 74	7.87	4.32
1L			L1+L2	1.080		0.918		13.880±272	14.792±238	33.879±644		
2		col clear + w tur	R	7.330	0.0101	1.069	0.5247±21	13.995± 14	14.756± 20	33.918± 58	7.90	4.32
3		col clear	R	2.247	0.0036	1.133	0.1762±38	13.840± 16	14.734± 20	33.756± 58	7.91	4.30
4		col clear	R	3.430	0.0060	1.207	0.269± 14	13.822± 28	14.707± 30	33.646±120	7.86	4.21
5	KV-454	col cl	R	2.205	0.0017	0.832	0.1097±48	13.768± 32	14.716± 36	33.660±108	7.89	4.27
5L			L1+L2	1.060		0.856		13.808±234	14.731±226	33.737±618		
6		col clear	R	7.389	0.0021	0.862	0.1356±16	13.823± 12	14.749± 16	33.764± 52	7.95	4.33
7	KV-570	col clear	R	1.208	0.0043	0.395	0.599 ±36	13.941± 50	14.746± 48	33.882±190	7.90	4.33
7L			L1+L2	0.910	0.0015	0.364	0.22 ±19	13.881±194	14.746±202	33.843±534		
8		col clear	R	6.300	0.0028	0.637	0.2476±64	15.208± 16	14.992± 20	35.099± 76	7.99	4.34
9	122-6	Pyrrhotite		>100				15.840± 13	15.159± 18	35.730± 43	8.14	4.36
10	80-3	Pyrrhotite		>100				17.373± 14	15.479± 18	37.418± 45	8.30	4.49
11	K501-12	Pyrrhotite		>100				15.043± 13	15.063± 18	34.951± 42	8.20	4.35
12	91-3	Pyrrhotite		>100				14.533± 12	15.007± 18	34.370± 41	8.25	4.27
13	K508-4	Pyrrhotite		>100				14.680± 12	15.052± 18	34.604± 42	8.30	4.35
Tsipringa intrusion												
14	C-110	col clear shiny	R	3.136	0.0003	0.999	0.0143±32	13.777± 12	14.738± 18	33.627± 52	7.93	4.23
14L			L1+L2	0.440	0.0021	1.095	0.106 ±18	13.862± 50	14.756± 50	33.747±126		
15		col clear	R	4.292	0.0005	1.283	0.0208±16	13.770± 12	14.748± 18	33.646± 52	7.96	4.26
16	C-103-3	col clear	R	6.985	0.0011	1.558	0.0401±10	13.900± 12	14.775± 18	33.749± 54	7.97	4.24
16L			L1+L2	0.360	0.0053	2.012	0.146 ±17	14.071± 50	14.832± 50	33.989±124		
17	C-113-3	col clear	R	2.641	0.0004	1.335	0.0182±28	13.763± 16	14.745± 20	33.660± 62	7.95	4.28
17L			L1+L2	0.020	0.0130	7.443	0.010 ± 6	14.043± 84	14.800± 58	33.920±158		
18		bulk fraction	R	17.799	0.0031	1.564	0.1107±38	13.983± 18	14.809± 22	33.865± 62	8.02	4.27
19	OI-1	Chalcopyrite		>100				14.760± 12	15.018± 18	35.116± 42	8.20	4.71
Lukkulaisvaara intrusion												
20	Lu-146/7	Translucent	R	1.229	0.0054	0.513	0.587 ±15	14.271± 36	14.857± 36	34.368± 98	8.02	4.49
21		col clear	R	10.019	0.0066	0.969	0.375 ±28	14.183± 28	14.814± 30	34.073±122	7.96	4.29
22	Lu-149	Translucent	R	5.210	0.0137	0.783	0.9734±12	14.219± 12	14.939± 18	34.147± 54	8.21	4.33
23		Translucent	R	1.513	0.0129	0.953	0.7511±78	14.259± 28	14.893± 28	34.004± 90	8.10	4.16
24		Chalcopyrite		1.075	0.0006	5.583	0.0057±15	14.443± 12	15.003± 18	34.304± 52	8.27	4.28
25		Pyrrhotite		0.906	0.0035	3.494	0.0562±52	14.625± 28	14.994± 30	34.854± 80	8.19	4.61
26	Lu-305/1	col clear + w tur	R	6.020	0.0068	3.827	0.0994±10	14.390± 12	14.941± 18	34.417± 54	8.16	4.43
27		col clear + w tur	R	0.868	0.0038	4.567	0.0476±22	14.800± 14	15.004± 18	34.719± 54	8.16	4.35
28		col clear + w tur	R	1.412	0.0048	3.908	0.0684±29	14.233± 26	14.882± 28	34.097± 88	8.09	4.27
29	Lu-314	Translucent	R	1.772	0.0021	1.300	0.0885±40	14.398± 18	14.920± 22	34.371± 70	8.11	4.38
30		col cl + w tur	R	0.945	0.0564	0.896	3.758 ±18	16.040± 22	15.183± 24	36.811± 68	8.12	4.96
31	Lu-610	Translucent	R	0.466	0.0019	0.573	0.178 ±33	14.064± 60	14.863± 50	34.014±130	8.10	4.34
32		col clear + w tur	R	1.244	0.0043	1.120	0.2155±70	14.338± 28	14.978± 30	34.287± 80	8.26	4.36
33	Lu-614	Translucent	R	5.770	0.0011	1.225	0.0502±16	13.945± 12	14.817± 18	33.902± 54	8.05	4.35
34		col clear	R	2.008	0.0007	1.107	0.033 ± 4	14.010± 18	14.825± 22	33.896± 60	8.04	4.28
35		Translucent	R	4.710	0.0017	0.754	0.1254±34	13.917± 26	14.741± 28	33.621± 82	7.89	4.10
36	Lu-617	col clear + w tur	R	2.768	0.0009	0.577	0.0829±72	13.957± 48	14.823± 48	33.855±122	8.06	4.29
37		translucent	R	13.620	0.0012	0.597	0.1076±12	13.971± 14	14.803± 18	33.816± 52	8.01	4.24
38	Lu-618	col clear + w tur	R	1.593	0.0014	1.550	0.0517±46	14.389± 16	14.850± 20	34.246± 58	7.97	4.27
39		col clear + w tur	R	0.914	0.0056	1.203	0.2624±90	14.629± 20	15.052± 22	34.382± 64	8.32	4.20
40	Lu-623	translucent	R	1.325	0.0013	0.795	0.090 ±10	13.984± 48	14.842± 50	33.890±136	8.09	4.30
41	Lu-300/2	Pyrrhotite		>100				17.642± 15	15.484± 18	37.446± 45	8.22	4.36
42	Lu-608/1	Pyrrhotite		>100				14.743± 12	15.006± 18	34.725± 42	8.18	4.40

Fractions 9-13, 19 ,41 and 42 are analyzed at the IPGG. Isotopic ratios are corrected for fractionation of 0.0013±0.0003 amu^{-1}. Errors (2σ) are based on external reproducibility of standard analyses.

All other fractions are analyzed at the ROM. Pb isotopic ratios are corrected for fractionation and procedure blank. Errors in $^{238}U/^{204}Pb$ and Pb isotopic ratios are 2σ, propagated to include within-run errors, reproducibility of fractionation coefficients, uncertainty in blank correction, and uncertainty of the Daly mass-discrimination coefficient for the measurements using Daly photomultiplier.

Fraction description. Plagioclase appearance: col-colorless, w-white, brn-brown, col cl + w tur- colorless clear crystals (fragments) with white turbid zones.

Leaching: L1-HCl leachate, L2-HNO_3 leachate, L1+L2-combined HCl and HNO_3 leachates, R-residue after acid leaching.

μ_1* is the model single-stage $^{238}U/^{204}Pb$ from T_E=4.55 Ga to T_C (see text for details).

κ* is the model single-stage $^{232}Th/^{238}U$ from T_E=4.55 Ga to T_C (see text for details).

The results of the leaching experiments show that: (1) Uranium and radiogenic Pb are preferentially removed by acid leaching of plagioclase as was demonstrated for K-feldspars (Ludwig and Silver, 1977; Gariépy and Allègre, 1985; McNaughton and Bickle, 1987). (2) The contrasting behavior of the U-Pb and Pb isotopic systems suggests that the apparent disturbance of the U-Pb system is a result of fractionation of U and Pb during leaching. The U/Pb ratios in acid washed plagioclase may thus be biased and should not be used for in situ decay correction in attempt to calculate initial Pb ratios. (3) More than one component of noninitial Pb is possibly present in plagioclase. One of these is a radiogenic Pb associated with a U-bearing phase, that remained a closed system since the time of crystallization. A

Table 2. U-Pb data for plagioclase fractions from the Burakovka Complex

Fraction number	Sample	Fraction description	Leaching	Fraction wt, mg	U ppm	Pb Ppm	$^{238}U/^{204}Pb$	$^{206}Pb/^{204}Pb$	$^{207}Pb/^{204}Pb$	$^{208}Pb/^{204}Pb$	μ_1*	κ*
43	4/38.9	brn translucent	R	9.499	0.0017	1.525	0.0613±12	14.355± 26	15.104± 28	34.231± 74	8.52	4.29
43L1			L1	0.658	0.0465	0.552	5.051 ±52	16.467± 58	15.447± 52	36.479±134		
43L2			L 2	0.039	0.4307	7.023	3.630 ±51	16.028± 58	15.361± 52	36.096±134		
44		col clear	R	6.460	0.0020	1.333	0.0829±22	14.359± 28	15.118± 32	34.301± 80	8.55	4.35
44L1			L 1	0.175	0.0084	2.372	0.214 ±23	16.917± 56	15.445± 50	36.911±132		
44L2			L 2	0.071	0.2003	9.193	1.367 ±28	17.878± 62	15.632± 54	38.089±142		
45		brn translucent	R	12.740	0.0025	1.290	0.1075±10	14.374± 12	15.091± 18	34.240± 56	8.49	4.28
46	4/192	col clear shiny	R	10.030	0.0001	1.544	0.0039 ± 8	14.343± 14	15.120± 20	34.203± 56	8.56	4.28
46L1			L 1	0.129	0.0102	1.176	0.494 ±58	14.946± 72	15.175± 56	34.747±156		
47		col clear shiny	R	14.540	0.0005	2.392	0.0123± 3	14.327± 12	15.086± 18	34.120± 50	8.49	4.21
48	45/186.4	brn translucent	R	6.689	0.0033	2.798	0.0660 ± 8	14.455± 12	15.138± 16	34.293± 56	8.56	4.26
48L1			L 1	0.035	0.0045	2.217	0.115 ±75	14.971±110	15.185± 62	34.793±168		
48L2			L 2	0.094	0.0127	0.759	0.96 ±13	15.565±108	15.324± 66	35.472±172		
49	31/185	brn translucent	R	2.097	0.0070	4.821	0.0805 ± 8	14.050± 12	14.977± 16	33.948± 50	8.36	4.30
50		brn translucent	R	3.890	0.0110	4.650	0.1310± 9	14.071± 12	14.967± 18	33.912± 52	8.33	4.24
51	31/300.3	brn translucent	R	2.727	0.0031	2.850	0.0581±12	13.383± 10	14.720± 16	33.290± 48	8.04	4.26
52		bulk fraction	R	11.110	0.0061	3.323	0.1002± 6	13.834± 10	14.801± 16	33.736± 50	8.06	4.29
53		brn translucent	R	2.640	0.0032	2.766	0.0617±13	13.394± 10	14.717± 16	33.281± 50	8.03	4.24
54	67/220.4	brn translucent	R	2.728	0.0056	3.089	0.1014±12	14.474± 12	15.148± 18	34.357± 52	8.58	4.30
55		col clear	R	2.667	0.0004	3.501	0.0072±10	14.424± 20	15.135± 24	34.312± 64	8.57	4.31
56		col clear	R	17.630	0.0090	2.972	0.1699± 8	14.535± 10	15.161± 16	34.433± 50	8.58	4.32

All fractions are analyzed at the ROM. See notes to Table 1 for the details.

Fraction numbering continues from Table 1.

Sm-Nd and Rb-Sr data for fraction 52: Sm-0.124 ppm, Nd-1.135 ppm, $^{147}Sm/^{144}Nd$=0.0664, $^{143}Nd/^{144}Nd$=0.510134±0.000011, $\varepsilon_{Nd}(2449)$=-7.8±0.5, Rb-2.70 ppm, Sr-732 ppm, $^{87}Rb/^{86}Sr$=0.0107, $^{87}Sr/^{86}Sr$=0.702951±18, $^{87}Sr/^{86}Sr(2449)$=0.702574±48.

Sm-Nd and Rb-Sr data for fraction 53: Sm-0.116 ppm, Nd-1.014 ppm, $^{147}Sm/^{144}Nd$=0.0695, $^{143}Nd/^{144}Nd$=0.510192±0.000025, $\varepsilon_{Nd}(2449)$=-7.7±0.8, Rb-1.46 ppm, Sr-719 ppm, $^{87}Rb/^{86}Sr$=0.0059, $^{87}Sr/^{86}Sr$=0.702845±11, $^{87}Sr/^{86}Sr(2449)$=0.702638±41.

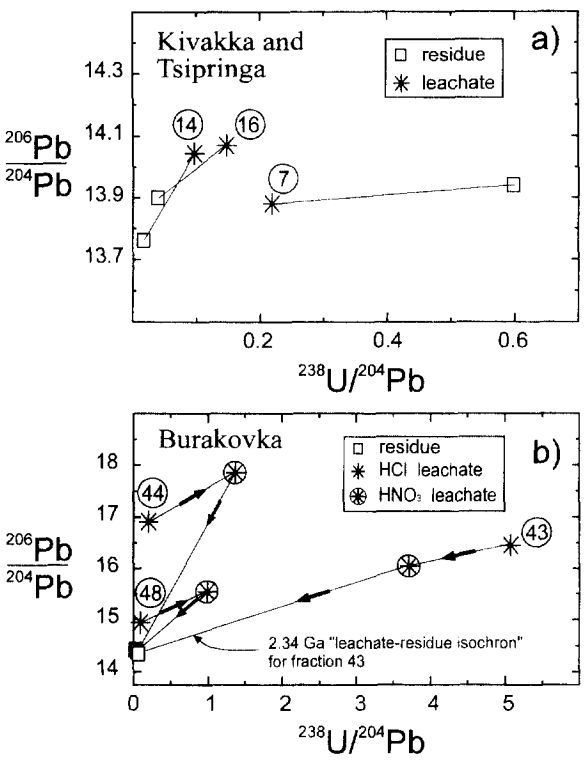

Fig. 2. $^{238}U/^{204}Pb$ vs. $^{206}Pb/^{204}Pb$ diagrams for acid leachates and residues of plagioclases from the Olanga (a) and Burakovka (b) complexes, showing fractionation of U and Pb during leaching. Encircled numbers indicate fraction numbers in Tables 1 and 2.

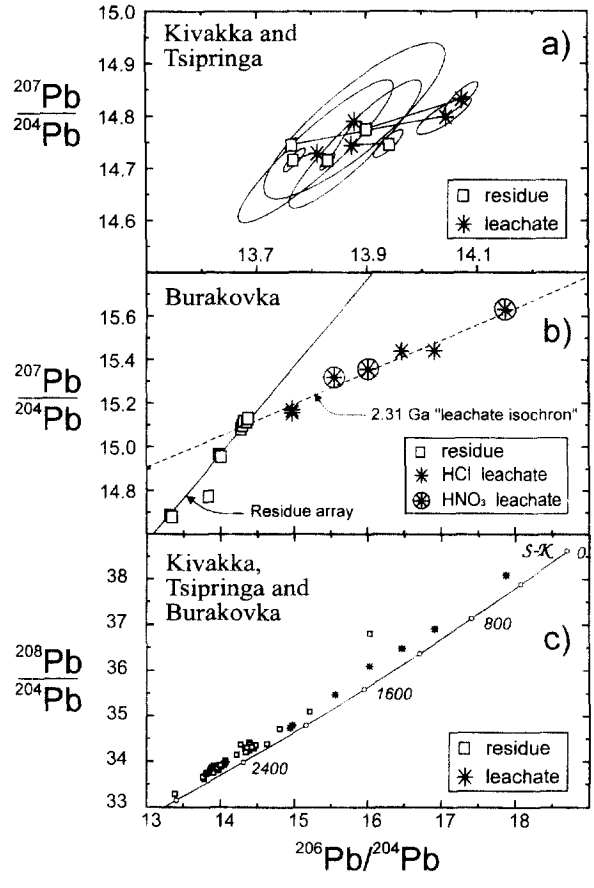

Fig. 3. Pb isotopic compositions of acid leachates and residues of plagioclases from the Olanga and Burakovka complexes. Error ellipses are plotted at 2σ. "Leachate isochron" is propagated through all seven leachate data points from Burakovka. Reference growth curve in the $^{208}Pb/^{204}Pb$-$^{206}Pb/^{204}Pb$ plot (c) is average crust after Stacey and Kramers (1975).

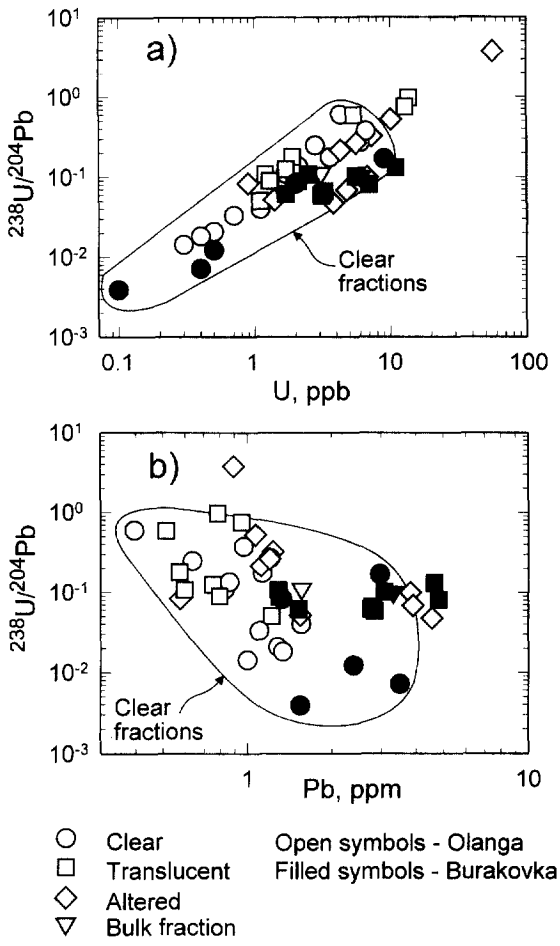

Fig. 4. Variations of measured $^{238}U/^{204}Pb$ in acid washed plagioclases vs. U and Pb concentrations. The outlined areas show U and Th variations in clear fractions. This diagram demonstrates that the lowest U concentrations (<1 ppb) are found in clear plagioclase fractions, while the higher U concentrations between 10 and 100 ppb are observed in translucent and altered fractions. Olanga plagioclases have commonly lower and more variable Pb concentrations than Burakovka plagioclases.

similar component was previously identified in K-feldspars (Ludwig and Silver, 1977; Gariépy and Allègre, 1985; Housh and Bowring, 1991).

4.2. Plagioclase and Sulfide U-Pb Data

Pb concentrations in acid-leached plagioclases vary between 0.4 and 5 ppm; the range of variations of U concentrations is from 0.1 and 56 ppb. The measured μ values vary within 3 orders of magnitude, from 0.004 to 3.8. The Burakovka plagioclases have commonly higher Pb concentration and lower U and measured μ values than the Olanga plagioclases (Fig. 4); however, the ranges of Pb and U concentrations in the Olanga and Burakovka plagioclases largely overlap. Strong positive correlation between μ and U concentration and only weakly negatively correlated μ and Pb concentrations (Fig. 4a,b) implies that the observed range of μ are chiefly a result of U variations. The U and Pb concentrations and $^{238}U/^{204}Pb$ ratio in the two Lukkulaisvaara sulfide fractions are within the range of plagioclase data.

The Pb isotopic compositions in plagioclase and sulfide fractions are plotted in Fig. 5, together with reference single-stage growth curves. In a $^{207}Pb/^{204}Pb$-$^{206}Pb/^{204}Pb$ diagram (Fig. 5a), most of the plagioclase data from the Olanga intrusions: Kivakka, Tsipringa, and Lukkulaisvaara plot as a scattered array with steeper slope than that of the 2.45 Ga reference isochron. Plagioclases from the Lukkulaisvaara intrusion have more radiogenic Pb and a wider range of isotopic variations than those from Kivakka and Tsipringa. The Olanga sulfide data plot along an a line with the slope m = 0.160, corresponding to an age of 2455 Ma, close to the crystallization age. This suggests the presence of significant in situ radiogenic component, accumulated since 2.45 Ga. The Olanga sulfide array intersects the upper ending of the Olanga plagioclase array at $^{206}Pb/^{204}Pb \approx 14.6$, $^{207}Pb/^{204}Pb \approx 15.0$. Both plagioclase and sulfide were analyzed from the Lukkulaisvaara gabbronorite Lu-149. The measured Pb isotopic compositions in chalcopyrite and pyrrhotite from that sample are more radiogenic than in plagioclase fractions, while the measured μ is lower in the sulfides than in the plagioclase.

The Burakovka plagioclase data plot along a linear array, approximately parallel to the Olanga plagioclase array, but having higher $^{207}Pb/^{204}Pb$ at a given $^{206}Pb/^{204}Pb$. The scatter of

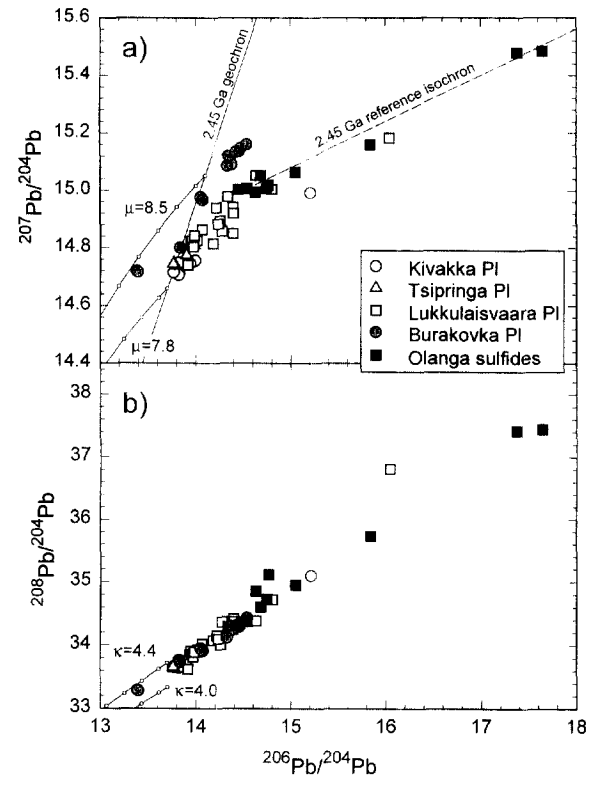

Fig. 5. Pb isotopic variations in acid washed plagioclase and sulfide fractions from Olanga and Burakovka complexes (data from Tables 1 and 2). Regression through all Olanga sulfide data is shown with the stippled line. Single-stage evolution curves shown for start at 4.55 Ga from primordial Pb isotopic composition (Tatsumoto et al., 1973). Evolution curves on the $^{208}Pb/^{204}Pb$-$^{206}Pb/^{204}Pb$ diagram (b) are calculated using $^{238}U/^{204}Pb$ (μ) of 7.8.

the data points is much less that for the Olanga. The only analytical point that substantially deviates from this array is the bulk plagioclase fraction 52 (Table 2), one of the two mineral fractions in this study that were not purified by handpicking.

In the $^{208}Pb/^{204}Pb$-$^{206}Pb/^{204}Pb$ diagram (Fig. 5b) plagioclases from Olanga and Burakovka, except the Lukkulaisvaara fraction 30 with high measured μ, plot along a single linear trend. The sulfide data follow the same trend but extend towards more radiogenic values, thus supporting the possible presence of radiogenic Pb in sulfides.

4.3. Plagioclase Sm-Nd and Rb-Sr Data

A number of plagioclase fractions studied here for U-Pb were also analyzed for Sm-Nd and Rb-Sr. Most of these results were reported by Amelin and Semenov (1996), and new data for two fractions from the Burakovka gabbronorite 31/300.3 are given in the footnote of Table 2. Initial ϵ_{Nd} in the Olanga Complex vary within the range of -0.6 to -2.2, only marginally exceeding analytical uncertainty. The range of $\epsilon_{Nd}(T)$ in the Burakovka is much larger, from -0.7 to -7.8. Apparent initial $^{87}Sr/^{86}Sr(T)$ vary between 0.7010 and 0.7028 in the Olanga and between 0.7026 and 0.7039 in the Burakovka. Initial $^{87}Sr/^{86}Sr(T^*)$ for the Olanga Complex, corrected for metamorphic Rb addition (Amelin and Semenov, 1996), are within 0.7017–0.7030.

5. DISCUSSION

5.1. Initial Lead Ratios in Plagioclase and the Role of Post-Crystallization Alteration

Before the plagioclase and sulfide Pb isotopic data can be used to constrain petrogenetic models, we must thoroughly evaluate all possible effects of disturbance and apply well-proven corrections or exclude the data to which such corrections cannot be applied. Pb in feldspars from igneous rocks may include several isotopically distinct components (Ludwig and Silver, 1977; Gancarz and Wasserburg, 1977; Gariépy and Allègre, 1985; McNaughton and Bickle, 1987; Housh and Bowring, 1991): initial Pb, incorporated into minerals during crystallization; radiogenic Pb, accumulated by in situ U and Th decay from the time of crystallization until present (radiogenic component), and, possibly, several other components introduced from other minerals and/or fluids during post-crystallization alteration or metamorphism (alteration components).

To our knowledge, there is no single analytical or theoretical approach that allows us to determine initial Pb composition if both radiogenic and alteration components are present. Acid leaching and vacuum volatilization (Sinha, 1969; Ludwig and Silver, 1977) can reduce these components but cannot guarantee their complete removal. The application of the model of dispersive isochronism (Tera, 1981) is limited to the cases with no initial isotope heterogeneity where minerals or leachates and residues form linear arrays in $^{207}Pb/^{204}Pb$-$^{206}Pb/^{204}Pb$ coordinates, but do not show linearity in $^{208}Pb/^{204}Pb$-$^{206}Pb/^{204}Pb$ plot. As our leaching experiments have shown, the proportion of radiogenic Pb in the plagioclases is decreased by acid leaching. We further attempt to distinguish the remaining radiogenic and alteration components from each other and from initial Pb.

The main problem with correction for a radiogenic Pb component in an acid-leached plagioclase is that U and Pb can easily fractionate during leaching, so that the measured μ is likely to be biased. In addition, a possible natural alteration may not only change the Pb isotopic composition of plagioclase, but also modify U/Pb ratios. Correction for the intrinsic U decay in acid-leached plagioclase can, therefore, yield wrong and misleading values and should not be used. In order to minimize the contribution from U-bearing phases, incompletely removed by leaching, we shall disregard all plagioclase analyses with measured μ larger than the arbitrarily chosen value of 0.3. This approach does not account for unsupported radiogenic Pb left after preferential removal of U by leaching. This component is considered together with alteration-related Pb in the subsequent discussion.

Alteration components are still more difficult to recognize and eliminate. The evidence for complex disturbance of Pb isotopic systems in the Olanga plagioclases is provided by analyses of optically different populations of plagioclase grains from the same sample. Internal isotopic variations can only result from variable contribution of radiogenic and alteration components, since the initial Pb isotopic composition is identical. The Pb isotopic data for the samples with significant internal isotopic variations are shown on Fig. 6. Plagioclase fractions from some samples: KV-570, C-113-3, Lu-305/1, and Lu-314, scatter along the 2.45 Ga reference isochron, implying the presence of variable amount of radiogenic component.

The other samples, Lu-610, Lu-614, and Lu-618, reveal more complex patterns of internal isotopic variations. Plagioclase populations in these samples show relatively large variations in $^{207}Pb/^{204}Pb$ and plot along the main Olanga plagioclase array (Fig. 5a). These variations are probably related to Pb redistribution during regional greenschist facies metamorphism in northern Karelia at ca. 1.75 Ga. The alteration component, which is likely to be even more variable between samples than between mineral grains in a sample, may be responsible for a part of the observed isotopic variations in the Olanga Complex.

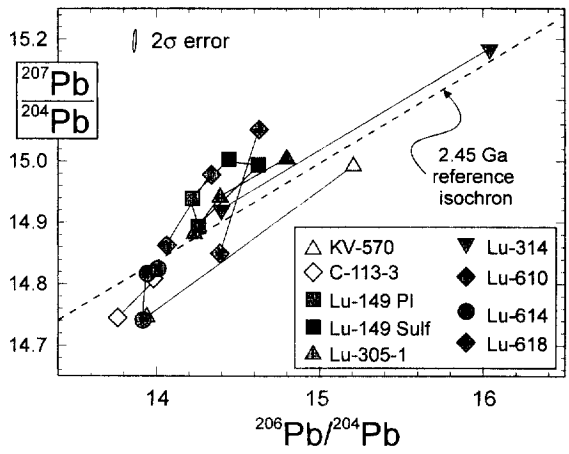

Fig. 6. Internal variations of measured Pb isotopic ratios in the Olanga plagioclases between optically distinct populations of plagioclase grains. Only samples with significant (outside 2σ error limits) internal variations in $^{206}Pb/^{204}Pb$ and $^{207}Pb/^{204}Pb$ are included. Two sulfide analyses from Lu-149 are also shown.

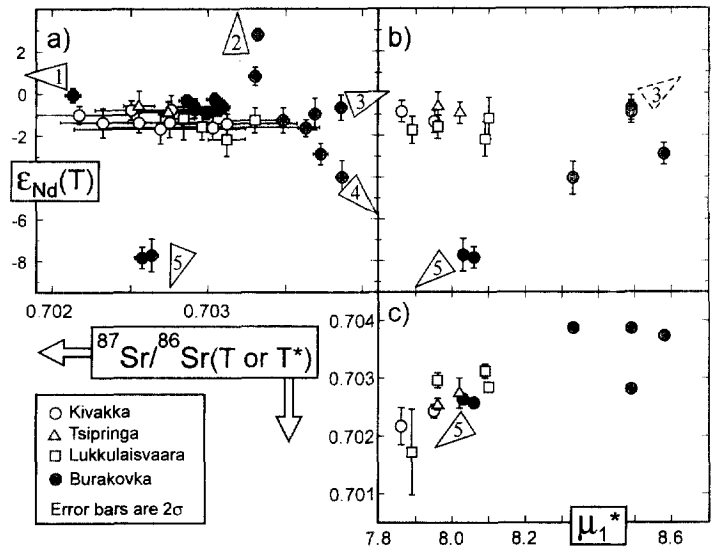

Fig. 7. (a) $\epsilon_{Nd}(T)$ vs. $^{87}Sr/^{86}Sr(T)$ diagram for the Olanga and Burakovka complexes, modified from Amelin and Semenov (1996) with addition of data for the Burakovka sample 31/300.3. Arrows with numbers indicate approximate directions towards suggested Burakovka mixing endmembers discussed in the text; (b,c) covariation between average time-integrated $^{238}U/^{204}Pb$ (μ_1*) in the Olanga and Burakovka sources, calculated from plagioclase Pb data (see text for details), with initial Nd and Sr isotopic ratios. Initial Nd and Sr isotopic values are from Table 2 (footnote) and from Amelin and Semenov (1996); μ_1* values are from Tables 1 and 2. Initial $^{87}Sr/^{86}Sr(T^*)$ for the Olanga Complex are corrected for metamorphic Rb addition as described by Amelin and Semenov (1996).

The Burakovka plagioclases (with the exception of bulk fraction #52) form a linear trend (Fig. 5a) with little excess scatter (MSWD = 2.8) and show little indication for complex post-crystallization disturbance. Evidence for closed-system behavior of Pb isotopic systems in the Burakovka is supported by the following observations: (1) no evidence for metamorphism in the Vodlozero block after the Burakovka emplacement; (2) concordant or nearly concordant zircons in the Burakovka gabbronorites (Amelin et al., 1995); and (3) internal Pb isotopic variations between optically different plagioclase populations reveal small radiogenic component in some samples (e.g., 67/220.4) and show no detectable alteration component in any of the analyzed samples. All Burakovka plagioclases have measured $\mu \leq 0.17$, so the contribution of a possible residual U-bearing phase is very small. Since the contributions of both alteration and radiogenic components are small, we interpret the bulk of Pb isotopic variations in Burakovka as initial isotopic heterogeneity.

5.2. Sources of Magmatism: Olanga Complex

Model $^{238}U/^{204}Pb$ (μ) and $^{232}Th/^{238}U$ (κ) values, calculated from the measured Pb isotopic compositions in the Olanga plagioclases and sulfides, are presented in Table 1. The single-stage $^{238}U/^{204}Pb$ ratios in the sources are calculated from projection of measured Pb isotopic compositions on T_E-T_C geochron along T_C secondary isochrons (T_E = 4.55 Ga is the assumed age of the Earth; T_C is the crystallization age determined from U-Pb zircon dating; primordial Pb isotopic composition after Tatsumoto et al., 1973). These values, denoted μ_1*, represent the average $^{238}U/^{204}Pb$ of mantle and crustal components, integrated over the period from T_E to T_C (Arndt and Todt, 1994), and might be also modified by the presence of alteration component. The κ* values are single-stage $^{232}Th/^{238}U$ ratios, integrated over the period from T_E to T_C.

The time-integrated $^{238}U/^{204}Pb$ (μ_1* values) in the Olanga intrusions vary from 7.86 to 8.32. The lower values around 7.9, typical for the Kivakka plagioclases, are close to the single-stage μ* = 7.7–7.9 in the abitibi mafic-ultramafic volcanoes, emplaced through juvenile 2.8–2.7 Ga crust (Dupré and Arndt, 1990, recalculated to T_E=4.55 Ga; Vervoort et al., 1994, Carignan et al., 1995b), which are not contaminated by a much older crust and are thought to be representative of the Archean depleted mantle. Similar μ_1* = 7.86 was determined in the 2.94 Ga Hautavaara greenstone belt, central Karelia (Ovchinnikova et al., 1994), which also has a depleted mantle Nd signature (S. Sergeev, pers. commun.).

Although the Pb isotopic composition in the Kivakka plagioclases is consistent with the depleted mantle source, the Nd and Sr isotopic systematics (Fig. 7) indicate the presence of substantial enriched component with low Sm/Nd and elevated Rb/Sr time-integrated ratios. Bulk contamination of a depleted mantle-derived magma with country rocks as the main cause of negative $\epsilon_{Nd}(T)$ in the Olanga Complex has been ruled out by Amelin and Semenov (1996) on the basis of mixing modeling with Nd and Sr isotopic data. The two alternative interpretations suggested by Amelin and Semenov (1996) for the Sr and Nd isotopic systematics of the Olanga and Burakovka complexes are the mantle plume source of magmatism with minor crustal contamination and the melting of an enriched lithospheric mantle source. The Pb isotopic systematics of the two complexes places additional constraints on the possible involvement of plume-derived material in the magmatism. If a single plume pro-

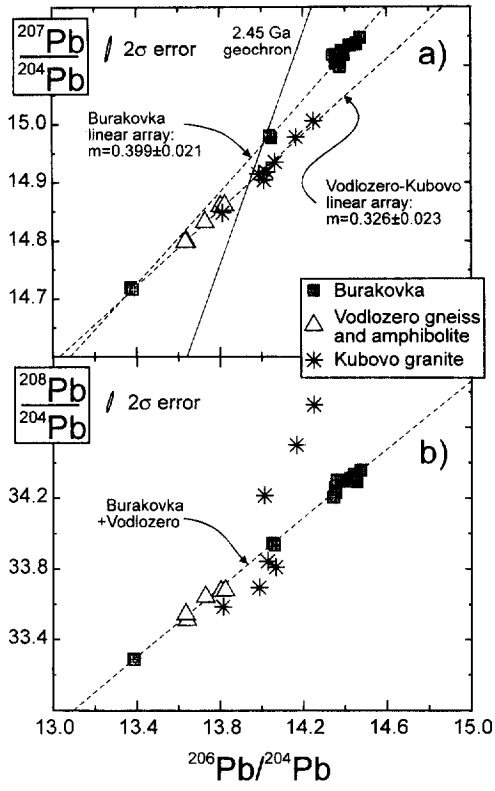

Fig. 8. Comparison between feldspar Pb ratios in Burakovka and Archean mafic to felsic rocks in the Vodlozero block. Data for the Vodlozero block gneisses and amphibolites are from Sergeev et al. (1990) and for the Kubovo granites from Ovchinnikova et al. (1991).

moted magma generation at 2.45–2.44 Ga throughout Baltic Shield, as suggested by Heaman (1997), then the plume-derived material would constitute a common mantle component in Olanga and Burakovka. However, the distinct fields of Pb isotopic compositions in these two complexes (Fig. 5a) argue against significant involvement of a common component in the magmatism. We must thus conclude that if a single plume component was present, its isotopic signature was overwhelmed by that of overlying lithosphere at least in one of the studied complexes.

Crustal contamination may still be responsible for the isotopic variations between and within intrusions of the Olanga Complex. Correlated variations in Pb, Sr, and Nd isotopic parameters (Fig. 7) can provide insights to the role of possible mechanisms of contamination. The $\epsilon_{Nd}(T)$ in the Olanga plagioclases show no statistically significant variations (Fig. 7a,b), while $^{87}Sr/^{86}Sr(T^*)$ and μ_1^* are positively correlated (Fig. 7c). This pattern may be explained by variable contamination with a partial melt from host rocks, with the larger amount of contamination in the Lukkulaisvaara intrusion. Alternatively, the isotopic variations could result from interaction of crystallizing Olanga intrusions with a fluid equilibrated with country rocks, which may also be responsible for the formation of sulfide mineralization in the Lukkulaisvaara intrusion (Semenov et al., 1994). Several lines of evidence suggest the link between late-magmatic fluid exchange, sulfide mineralization, and Pb and Sr isotopic variations: (1) Higher μ_1^* in sulfides from Lu-149 compared to plagioclase; (2) Higher μ_1^* and $^{87}Sr/^{86}Sr(T^*)$ in plagioclases are observed in the Lukkulaisvaara intrusion, in which the late-magmatic to post-magmatic metasomatism is more pronounced than in Kivakka and Tsipringa intrusions (Semenov et al., 1994, and Semenov, pers. commun.); (3) Elevated μ_1^* in sulfides from the Kivakka and Tsipringa intrusions, compared to plagioclase; and (4) Lack of Nd isotopic variations, consistent with relatively low solubility of REE in aqueous fluids (e.g., Hajash, 1984; Michard and Albarède, 1986). Internal Pb isotopic variations in the Lukkulaisvaara samples Lu-610, Lu-614, Lu-618, approximately parallel to the Olanga linear array, may also be related to the same process. The above observations cannot be explained by magma contamination, and we, therefore, consider the late-magmatic to post-magmatic open-system fluid exchange as the most likely cause of isotopic variations in the Olanga Complex.

5.3. Sources of Magmatism: Burakovka Complex

Isotopic data for the Burakovka Complex indicate involvement of multiple components of possible crustal and mantle origin. Although linear $^{207}Pb/^{204}Pb$-$^{206}Pb/^{204}Pb$ correlation (Fig. 5a) is consistent with simple binary mixing, the more extensive Sr and Nd isotopic dataset (Fig. 7a; Amelin and Semenov, 1996) suggests that at least five isotopically distinct components were involved. Of course, these components are not necessarily independent, but might have been derived from a smaller number of initial endmembers through various processes (Amelin and Semenov, 1996). The distribution of data in μ_1^* vs. initial Sr and Nd isotopic ratios plots (Fig. 7b,c) does not reproduce the distinction between components identified in $\epsilon_{Nd}(T)$ vs. $^{87}Sr/^{86}Sr(T)$ space. This suggests that some processes during assimilation, magma mixing, or earlier protolith evolution have probably decoupled U-Pb isotopic system from Rb-Sr and Sm-Nd.

In order to identify some of the mixing endmembers, the Burakovka plagioclase Pb isotopic data are compared with published Pb isotopic data for various Archean rocks in the Vodlozero block. We do not imply that the gneisses, amphibolites, and granites, exposed in the Vodlozero block, are representative of all possible Burakovka contaminants. However, the Burakovka parental magmas have been in contact with the Vodlozero crustal rocks, and this is a sufficient reason to consider the latter among plausible contaminants.

Plagioclase and K-feldspar Pb in the Vodlozero amphibolites and amphibolite-facies gneisses (Sergeev et al., 1990) and the Kubovo late-kinematic granites (Ovchinnikova et al., 1991) are shown on Fig. 8 together with the Burakovka plagioclase data. The Pb isotopic systems in minerals of the Vodlozero rocks were equilibrated during the 2.54–2.48 Ga metamorphism (Sergeev et al., 1990; Ovchinnikova et al., 1991), so the Vodlozero feldspar Pb isotopic data can be directly compared with the Burakovka plagioclase data. In the $^{207}Pb/^{204}Pb$-$^{206}Pb/^{204}Pb$ diagram (Fig. 8a), Vodlozero and Kubovo data taken together plot on a linear trend with a slope m = 0.326 ± 0.023, distinctly lower than the Burakovka trend (m = 0.399 ± 0.021). Intersection of the trends shows that the Burakovka low-$^{207}Pb/^{204}Pb$ component, represented by sample 31/300.3

Table 3. Average single-stage time-integrated κ in Archean and early Proterozoic rocks.

Geological unit	Age, Ga	Mineral	κ* (±1 s.d.)	Data source
Baltic Shield				
Kivakka intrusion	2.445	Plag#)	4.29±0.05	This study
Tsipringa intrusion	2.441	Plag#)	4.26±0.02	This study
Lukkulaisvaara intrusion	2.442	Plag#)	4.30±0.08	This study
Olanga Complex average		Plag#)	4.29±0.07	This study
Burakovka Complex	2.449	Plag#)	4.28±0.04	This study
Vodlozero gneisses	2.50*)	KFSp+Plag#)	4.27±0.03	Sergeev et al. (1990)
Suomussalmi mafic volcanics	2.70	Galena	4.30±0.04	Vidal et al. (1980)
Superior Province				
Abitibi subprovince-mafic volcanics	2.70	Various sulfides	4.15±0.08	Brévart et al. (1986), Dupré & Arndt (1990)
		Galena	4.23±0.05	Franklin & Thorpe (1982)
Abitibi subprovince-granitoids	2.70	KFSp#)	4.17±0.06	Gariépy & Allègre (1985)
Mulcahy intrusion	2.78-2.73	Plag#)	4.17±0.13	Carignan et al (1995a)
Slave Province				
Mafic volcanics	2.70	Galena	4.21±0.07	Franklin & Thorpe (1982)
Churchill Province				
Mafic volcanics	2.70	Galena	4.29±0.05	Franklin & Thorpe (1982)
Yilgarn Craton (mafic volcanics)				
Murchison Province	3.00	Galena	4.31±0.09	Browning et al. (1987)
Southern Cross Province	3.00	Galena	4.26±0.07	Browning et al. (1987)
Norseman Wiluna Prov.	2.70	Galena	4.22±0.12	Browning et al. (1987)
E. Goldfields Province	2.90	Galena	4.30±0.07	Browning et al. (1987)
W.Greenland				
Amîtsoq gneisses	3.60*)	KFSp+Plag#)	4.26±0.08	Gancarz & Wasserburg (1977)
Bulk Earth estimates			4.2	Allègre et al. (1986)
			3.9±0.2	Rocholl & Jochum (1993)

*) Age of metamorphism

#) Only plagioclase and K-feldspar data with measured $^{238}U/^{204}Pb<0.3$ are included.

(component 5 in Fig. 7), may be similar to the Vodlozero amphibolite-facies crust. Position of this component and the Vodlozero feldspar data to the left of the geochron (Fig. 8a) implies that the U/Pb ratio in their protoliths was reduced long before 2.45 Ga, probably during metamorphic events at 3.15–2.86 Ga (Lobach-Zhuchenko et al., 1993). The similarity between the Burakovka low-$^{207}Pb/^{204}Pb$ component and the Vodlozero amphibolite-facies crust is supported by colinearity of Pb isotopic ratios in the $^{208}Pb/^{204}Pb$-$^{206}Pb/^{204}Pb$ diagram (Fig. 8b). The low $\epsilon_{Nd}(T)$ and $^{87}Sr/^{86}Sr(T)$ in this endmember (Fig. 7) advocate its origin from a Mesoarchean lower crust, and the Nd isotopic value is similar to those of Vodlozero gneisses and amphibolites (Lobach-Zhuchenko et al., 1993). The Pb isotopic data, both $^{207}Pb/^{204}Pb$-$^{206}Pb/^{204}Pb$ and $^{208}Pb/^{204}Pb$-$^{206}Pb/^{204}Pb$, argue against involvement of the upper crustal component, similar to the Kubovo granites, in the Burakovka magmatism.

The origin of endmembers with $\epsilon_{Nd}(T)$ of -1 to -3, $^{87}Sr/^{86}Sr(T) = 0.7028 - 0.7038$, and high μ_1* is more controversial. Nearly constant μ_1* of 8.50–8.58 in this group contrasts with the variability of initial Nd and Sr isotopic ratios. Unless the similarity of Pb isotopic ratios between several crustal contaminants is coincidental, the Burakovka data would imply a multistage contamination process, in which Pb, Sr, and Nd were decoupled. Assimilation of Vodlozero gneiss was probably a late-stage, local shallow-level process, that occurred by melting wallrock xenoliths in the magma chamber. This process had apparently little effect on the high-μ_1* group of rocks, except for causing small Pb isotopic variations along the main Burakovka trend in the $^{207}Pb/^{204}Pb$–$^{206}Pb/^{204}Pb$ coordinates. The medium-stage contamination could occur earlier in the magma chamber, as indicated by decreasing $\epsilon_{Nd}(T)$ upwards in the Burakovka layered series (Amelin and Semenov, 1996), and/or during magma ascent to the surface. Variations in initial ϵ_{Nd} and $^{87}Sr/^{86}Sr$ would have been created at this stage. The Pb isotopic composition would have been enriched and homogenized by this time, because no geological process we are aware of could create uniform Pb isotopic composition in the magmas without homogenizing Nd and Sr isotopic compositions as well.

An enriched high-μ_1* component had thus been brought into the Burakovka parental magmas or their source before the stage described above. The amount of Pb introduced during early enrichment must have been sufficiently large to make the parental magma insensitive to assimilation of crustal rocks, while the enrichment in Sr and Nd must have been smaller. Subduction zone fluid transfer is a highly efficient mechanism for selective Pb enrichment (Brenan et al., 1995; You et al., 1996), that can mobilize Pb from subducted sediments (e.g., Ishikawa and Nakamura, 1994). Our preferred explanation for the origin of the Burakovka high-μ_1* feature is that the parental magmas were derived from a high-μ enriched Archean mantle, modified by sediment subduction. This model is similar to those proposed by Wooden et al. (1991) and Amelin et al. (1996) to explain enriched isotopic signatures in the Stillwater and Dovyren layered complexes. High μ_1* = 8.67–8.75 (recalculated to T_E = 4.55 Ga), slightly higher than the Burakovka values, are determined in the komatiitic basalts, erupted in the Vetreny belt, adjacent to the Vodlozero block, contemporaneously with the Burakovka emplacement (Puchtel et al., 1997). These data suggest that subduction-related Pb enrichment was probably a regional feature of the mantle beneath southeastern Karelia in the early Proterozoic.

5.4. Uniformity of the Source Th/U Ratio in the Archean and the Earliest Proterozoic Crust-Mantle System

Single-stage $^{232}Th/^{238}U$ (κ^*), integrated over the period from T_E to T_C, are shown in Tables 1 and 2. The average κ^* between 4.27 and 4.30 (Table 3) are uniform for all studied intrusions and are similar to the value in the Vodlozero gneisses (calculated from the data of Sergeev et al., 1990). These values are identical to the model κ in Archean mantle (Allègre et al., 1986; Zartman and Haines, 1988) and are similar or marginally higher than the bulk Earth values (Allègre et al., 1986; Rocholl and Jochum, 1993). The compilation of average κ^* values for a number of Archean complexes (Table 3), based on Pb isotopic data for feldspar with little alteration and radiogenic components, and galena, suggests that the uniformity of time-integrated $^{232}Th/^{238}U$ ratios in Archean and the earliest Proterozoic is a global, rather than regional, phenomenon.

If the uniformity of $^{232}Th/^{238}U$ ratios in magma sources of both mantle and crustal origin, that underwent a complex history of U/Pb fractionation, is indeed a universal feature of Archean and the earliest Proterozoic rocks, it places strong constraints on mechanisms of the crust-mantle differentiation. This would imply that the large-scale differentiation occurred so that Pb was fractionated from U, but not Th from U. A mechanism of mantle differentiation and lithosphere growth without Th/U fractionation may be based on hydrothermal Pb transfer from oceanic crust to continent with high-Pb metalliferous sediments (Peucker-Ehrenbrink et al., 1994; Chauvel et al., 1995). Mass balance calculations of these authors have shown that this mechanism probably operated since early Archean (ca. 4 Ga), and was more efficient during Archean due to higher rates of production of oceanic crust (Hargraves, 1986). In addition, crustal weathering and sediment formation that strongly fractionate U from Th and Pb in the post-Archean oxidizing conditions (Asmerom and Jacobsen, 1993; Zartman and Haines, 1988), might have not done so during Archean, when atmosphere and hydrosphere contained no free oxygen (Holland, 1984; Kasting et al., 1993), and oxidation of U to water soluble hexavalent state was unlikely. Different Archean mantle and crustal reservoirs could thus acquire distinct U/Pb but similar Th/U ratios.

A number of processes that fractionate U, Th, and Pb came forth at latest Archean and early Proterozoic. Intracrustal melting with plagioclase as a residual phase (Taylor and McLennan, 1985) increases U/Pb in granitoid upper crust and decreases it in residual lower crust. A complementary process of foundering of lower crust (Arndt and Goldstein, 1989) decreases U/Pb and Sm/Nd in subcontinental mantle. Growing concentration of free oxygen in atmosphere and hydrosphere (Holland, 1984; Kasting et al., 1993) causes U oxidation during weathering, resulting in increase of U concentration in seawater and recycling of U into mantle with subducted slabs. All together, these processes changed Pb isotopic evolution from an Archean to a modern path, decreasing Th/U in the depleted mantle and leading in a long term to the discrepancy between present-day and time-integrated Th/U ratios (e.g., Galer and O'Nions, 1985).

In contrast to the uniformity of time-integrated $^{232}Th/^{238}U$ ratios in the magma sources, determined from initial Pb ratios, a wide range of Th/U ratios was derived from slopes of $^{208}Pb/^{204}Pb$-$^{206}Pb/^{204}Pb$ linear arrays for Archean and early Proterozoic komatiites and komatiitic basalts (Dupré et al., 1984; Brévart et al., 1986; Dupré and Arndt, 1990; Carignan et al., 1995b; Puchtel et al., 1997). Evaluation of the source $^{232}Th/^{238}U$ from $^{208}Pb/^{204}Pb$-$^{206}Pb/^{204}Pb$ linear arrays is based on consideration of Th/U ratios in komatiites as representative of their mantle sources. This is certainly a reasonable approach for komatiites that were not contaminated. However, the commonly used test for contamination, based on Nd and Pb isotopic compositions, is not universal. The depleted mantle-type isotopic signatures (i.e., high ϵ_{Nd} and low μ_1*) of many komatiites can indeed constrain comtamination by old continental crust, but even large amount of contamination by juvenile continental crust can have little or no effect on radiogenic isotope ratios. At the same time, chemical effects of crustal contamination depend on mechanism of contamination, proportion of mixing, and composition of contaminant, but not on the age of contaminant. Komatiites have enormous ability to assimilate crustal rocks (Huppert and Sparks, 1985; Lesher and Arndt, 1995) and very low starting concentrations of Th and U (Jochum et al., 1991), contrasting markedly with high Th and U contents in crustal rocks, therefore, the komatiite Th/U ratios can potentially be dominated by crustal contaminants in many cases. We think that any komatiites should be carefully examined using most sensitive chemical criteria of contamination, before their Th/U ratios are considered as the mantle source values. If Th/U ratios in komatiites are indeed representative of their local contaminants, then their wide range of variations is naturally explained by fractionation of granitoid magmas, involving high-U, Th minerals with highly contrasting Th/U (zircon, monazite, allanite, titanite etc.). These variations are, however, likely to be effectively averaged over the larger volumes of the crust.

6. CONCLUSIONS

The study of U-Pb systems in plagioclase and sulfide fractions from the Paleoproterozoic Olanga and Burakovka mafic layered complexes has a number of implications for the methodology of Pb isotopic studies of ancient mafic rocks and for U-Th-Pb fractionation in the Archean crust-mantle system.

Handpicking of pure homogeneous mineral fractions, acid leaching, and analyses of both Pb and U in leachates and residues are essential steps in a Pb isotopic study of ancient igneous rocks. Mild leaching in HCl and HNO_3 removes most of the uranium and radiogenic Pb from plagioclase. Uranium and Pb may be strongly fractionated during leaching, so the correction for in situ U decay should not be applied to acid leached plagioclases. Pb in plagioclase contains isotopically distinct initial, radiogenic, and alteration-related components. The alteration component is a product of U-Pb system disturbance during regional metamorphism and is reduced, but not necessarily completely removed by leaching. Plagioclases from unmetamorphosed mafic rocks yield more reliable initial Pb ratios. Sulfides were also found to contain a significant radiogenic component.

Pb isotopic compositions of plagioclases in the Olanga and Burakovka complexes plot along two different, approximately parallel trends in the $^{206}Pb/^{204}Pb$-$^{207}Pb/^{204}Pb$ diagram. The time-integrated single stage $^{238}U/^{204}Pb$ values in the sources of

the Olanga complex, intruding 2.8–2.7 Ga crust, spread from 7.86 to 8.32. Although the lower $^{238}U/^{204}Pb$, calculated for plagioclases from the Kivakka intrusion, is close to the depleted mantle value, combined Pb, Sr, and Nd isotopic systematics suggest either enriched lithospheric or slightly contaminated plume source. Internal Pb, Sr, and Nd isotopic variations in the Olanga Complex and higher $^{207}Pb/^{204}Pb$ sulfides compared to plagioclases are probably a result of late-magmatic fluid exchange with host rocks.

The Burakovka Complex, emplaced into the pre-3.1 Ga crust, shows a much higher time-integrated $^{238}U/^{204}Pb$ than the Olanga complex, as well as much larger variations in $\epsilon_{Nd}(T)$. Initial Pb, Sr, and Nd isotopic variations within Burakovka probably result from several subsequent processes: fluid-related enrichment that introduced sediment-derived Pb to the mantle magma sources was followed by assimilation of wallrock material during magma ascent and emplacement. Finally, local contamination by a crustal material, similar to amphibolite-grade country rocks, occurred in the magma chamber.

Time-integrated Th/U ratios are identical for sources of both complexes and are similar to the Archean mantle value, despite the significant difference in U/Pb. This implies that differentiation in Archean crust-mantle system occurred by processes that fractionated Pb from U, but not Th from U. The likely process is a hydrothermal Pb transfer, rather than magmatic intracrustal differentiation and U transfer in weathering cycle, typical for post-Archean.

Acknowledgements—Our thanks are due to V.Semenov and S.Turchenko, who provided plagioclase and sulfide separates for this study. We are grateful to G. Ovchinnikova and B. Gorokhovsky for analytical assistance at the IPGG. Cooperative efforts of the ROM Geochronology Lab staff made possible U-Pb analyses at a uniform low blank level. R. Zartman, F. Corfu, and I. Puchtel made valuable comments on the manuscript. Thorough reviews by J. Vervoort, C. Gariépy, and S. Shirey are greatly appreciated. Financial support was provided by an NSERC operating grant to the Geochronology Lab and a grant from Russian Academy of Sciences for advanced research.

REFERENCES

Alapieti T. T., Filen B. A., Lahtinen J. J., Lavrov M. M., Smolkin V. F., and Voitsekhovsky S. N. (1990) Early Proterozoic layered intrusions in the northeastern part of the Fennoscandian shield. *Mineral. Petrol.* **42**, 1–22.

Allègre J., Dupré B., and Lewin E. (1986) Thorium/uranium ratio of the Earth. *Chem. Geol.* **56**, 219–227.

Amelin Yu. V. and Semenov V. S. (1996) Nd and Sr isotope geochemistry of mafic layered intrusions in the eastern Baltic Shield: Implications for the sources and contamination of Paleoproterozoic continental mafic magmas. *Contrib. Mineral. Petrol.* **124**, 255–272.

Amelin Yu. V., Heaman L. M., and Semenov V. S. (1995) U-Pb geochronology of layered mafic intrusions in the eastern Baltic Shield: Implications for the timing and duration of Paleoproterozoic continental rifting. *Precamb. Res.* **75**, 31–46.

Amelin Yu. V., Neymark L. A., Ritsk E. Yu., and Nemchin A. A. (1996) Enriched Nd-Sr-Pb isotopic signatures in the Dovyren layered intrusion (eastern Siberia, Russia): Evidence for source contamination by ancient upper crustal material. *Chem. Geol.* **129**, 39–69.

Amelin Yu. V., Ritsk E. Yu., and Neymark L. A. (1997) Effects of interaction between ultramafic tectonite and mafic magma on Nd-Pb-Sr isotopic systems in the Neoproterozoic Chaya massif, Baikal-Muya ophiolite belt. *Earth Planet. Sci. Lett.* **148**, 299–316.

Arndt N. T. and Goldstein S. L. (1989) An open boundary between lower continental crust and mantle: Its role in crust formation and crustal recycling. *Tectonophysics* **161**, 201–212.

Arndt N. T. and Todt W. (1994) Formation of 1.9 Ga old Trans-Hudson continental crust: Lead isotope data. *Chem. Geol.* **118**, 9–26.

Asmerom Y. and Jacobsen S. B. (1993) The lead isotopic evolution of the Earth: Inferences from river water suspended loads. *Earth Planet. Sci. Lett.* **115**, 245–256.

Brenan J. M., Shaw H. F., and Ryerson F. J. (1995) Experimental evidence for the origin of lead enrichment in convergent-margin magmas. *Nature* **378**, 54–56.

Brévart O., Dupré B., and Allègre C. J. (1986) Lead-lead age of komatiitic lavas and limitations on the structure and evolution of the Precambrian mantle. *Earth Planet. Sci. Lett.* **77**, 293–302.

Browning P., Groves D. I., Blockley J. G., and Rosman K. J. R. (1987) Lead isotope constraints on the age and source of gold mineralization in the Archean Yilgarn Block, Western Australia. *Econ. Geol.* **82**, 971–986.

Buiko A. K., Levchenkov O. A., Turchenko S. I., and Drubetskoy E. R. (1995) Geology and isotopic dating of the early Proterozoic Sumi-Sariola Complex of northern Karelia (the Tsipringa-Panajarvi structure). *Stratigr. Geol. Correl.* **3**, 16–30.

Carignan J., Machado N., and Gariépy C. (1995a) Initial lead isotopic composition of silicate minerals from the Mulcahy layered intrusion: Implications for the nature of the Archean mantle and the evolution of greenstone belts in the Superior Province, Canada. *Geochim. Cosmochim. Acta* **59**, 97–105.

Carignan J., Machado N., and Gariépy C. (1995b) U-Pb isotopic geochemistry of komatiites and pyroxenes from the southern Abitibi greenstone belt, Canada. *Chem. Geol.* **126**, 17–27.

Chauvel C., Goldstein S. L., and Hofmann A. W. (1995) Hydration and dehydration of oceanic crust controls lead evolution in the mantle. *Chem. Geol.* **126**, 65–75.

Dupré B. and Arndt N. T. (1990) Lead isotopic compositions of Archean komatiites and sulfides. *Chem. Geol.* **85**, 35–56.

Dupré B., Chauvel C., and Arndt N. T. (1984) Lead and neodymium study of two Archean komatiitic flows from Alexo, Ontario. *Geochim. Cosmochim. Acta* **48**,, 1965–1972.

Franklin J. M. and Thorpe R. I. (1982) Comparative metallogeny of the Superior, Slave, and Churchill provinces. *Geol. Assoc. Canada Spec. Paper* **25**, 3–89.

Galer S. J. C. and O'Nions R. K. (1985) Residence time of thorium, uranium, and lead in the mantle with implications for the mantle convection. *Nature* **316**, 778–782.

Gancarz A. J. and Wasserburg G. J. (1977) Initial lead of the Amîtsoq gneiss, West Greenland and implications for the age of the Earth. *Geochim. Cosmochim. Acta* **41**, 1283–1301.

Gariépy C. and Allègre C. J. (1985) The lead isotope geochemistry and geochronology of late-kinematic intrusives from the Abitibi greenstone belt and the implications for late Archean crustal evolution. *Geochim. Cosmochim. Acta* **49**, 2371–2383.

Gorbunov G. I., Zagorodny V. G., and Robonen W. I. (1985) Main features of the geological history of the Baltic Shield and the epochs of ore formation. *Geol. Surv. Finland Bull.* **333**, 2–41.

Hajash A. (1984) Rare earth element abundances and distribution patterns in hydrothermally altered basalts: Experimental evidence. *Contrib. Mineral. Petrol.* **85**, 409–412.

Hargraves R. B. (1986) Faster spreading or greater ridge length in the Archean? Geology **14**, 750–752.

Heaman L. M. (1997) Global mafic magmatism at 2.45 Ga: Remnants of an ancient large igneous province? *Geology* **25**, 299–302.

Holland H. D. (1984) *Chemical Evolution of the Atmosphere and Oceans.* Princeton Univ. Press.

Housh T. and Bowring S. A. (1991) Lead isotope heterogeneities within alkali feldspars: Implications for determination of initial lead isotopic compositions. *Geochim. Cosmochim. Acta* **55**, 2309–2316.

Huppert H. E. and Sparks R. S. J. (1985) Cooling and contamination of mafic and ultramafic magmas during ascent through continental crust. *Earth Planet. Sci. Lett.* **74**, 371–386.

Ishikawa T. and Nakamura E. (1994) Origin of the slab component in arc lavas from cross-arc variation of B and Pb isotopes. *Nature* **370**, 205–208.

Jochum K. P., Arndt N. T., and Hofmann A. W. (1991) Nb-Th-La in komatiites and basalts: Constraints on komatiite petrogenesis and mantle evolution. *Earth Planet. Sci. Lett.* **107**, 272–289.

Kasting J. F., Eggler D. H., and Raeburn S. P. (1993) Mantle redox

evolution and the oxidation state of the Archean atmosphere. *J. Geol.* **101**, 245–257.

Leeman W. P. (1979) Partitioning of Pb between volcanic glass and coexisting sanidine and plagioclase feldspars. *Geochim. Cosmochim. Acta.* **43**, 171–175.

Lesher C. M. and Arndt N. T. (1995) REE and Nd isotope geochemistry, petrogenesis, and volcanic evolution of contaminated komatiites at Kambalda, Western Australia. *Lithos* **34**, 127–157.

Lobach-Zhuchenko S. B., Chekulayev V. P., Sergeev S. A., Levchenkov O. A., and Krylov I. N. (1993) Archaean rocks from southeastern Karelia (Karelian granite-greenstone terrain). *Precamb. Res.* **62**, 375–397.

Ludwig K.R. (1992) ISOPLOT - a plotting and regression program for radiogenic - isotope data, version 2.57. USGS Open-File Rept. 91-445.

Ludwig K. R. and Silver L. T. (1977) Lead isotope inhomogeneity in Precambrian igneous K-feldspars. *Geochim. Cosmochim. Acta* **41**, 1457–1471.

McNaughton N. J. and Bickle M. J. (1987) K-feldspar Pb-Pb isotopic systematics of Archaean post-kinematic granitoid intrusions of the Diemals area, central Yilgarn Block, Western Australia. *Chem. Geol. (Isot. Geosci. Sect.)* **66**,, 193–208.

Michard A. and Albarède F. (1986) The REE content of some hydrothermal fluids. *Chem. Geol.* **55**, 51–60.

Neymark L. A., Amelin Yu. V., and Larin A. M. (1994) Pb-Nd-Sr isotopic and geochemical constraints on the origin of the 1.54–1.56 Ga Salmi rapakivi granite-anorthosite batholith. *Mineral. Petrol.* **50**, 173–193.

Ovchinnikova G. V. et al. (1991) Geochemical and isotope data on the dating and petrology of southeast Karelian late-kinematic granites. *Geochem. Intl.* **28**, 35–47.

Ovchinnikova G. V., Matrenichev V. A., Levchenkov O. A., Sergeev S. A., Yakovleva S. Z., and Gorokhovsky B. M. (1994) U-Pb and Pb-Lead isotope studies of acid volcanics from the Hautavaara greenstone structure, central Karelia. *Petrol.* **2**, 230–243.

Oversby V. M. (1975) Lead isotope systematics and ages of Archaean acid intrusives in the Kalgoorlie-Norseman area, Western Australia. *Geochim. Cosmochim. Acta* **39**, 1107–1125.

Peuker-Ehrenbrink B., Hofmann A. W., and Hart S. R. (1994) Hydrothermal lead transfer from mantle to continental crust: The role of metalliferous sediments. *Earth Planet. Sci. Lett.* **125**, 129–142.

Puchtel I. S., Hofmann A. W., Mezger K., Shchipansky A. A., Kulikov V. S., and Kulikova V. V. (1996) Petrology of a 2.41 Ga remarkably fresh komatiitic basalt lava lake in Lion Hills, central Vetreny Belt, Baltic Shield. *Contrib. Mineral. Petrol.* **124**, 273–290.

Puchtel I. S. et al. (1997) Petrology and geochemistry of crustally contaminated komatiitic basalts from the Vetreny Belt, southeastern Baltic Shield: Evidence for an early Proterozoic mantle plume beneath rifted Archean continental lithosphere. *Geochim. Cosmochim. Acta* **61**, 1205–1222.

Rocholl A. and Jochum K. P. (1993) Thorium, uranium, and other trace elements in carbonaceous chondrites: Implications for the terrestrial and solar-system Th/U ratio. *Earth Planet. Sci. Lett.* **117**, 265–278.

Semenov V. S., Pchelintseva N. F., Ushen N., and Kotov N. V. (1994) Noble metal-bearing ore metasomatites of the Lukkulaisvaara layered intrusion, northern Karelia. *Vestnik St. Peterburg Univ. Ser. 7, Issue* **3**, 25–33 (in Russian).

Semenov V. S., Koptev-Dvornikov E. V., Berkovskii A. N., Kireev B. S., Pchelintseva N. F., and Vasil'eva M. O. (1995) Layered troctolite-gabbro-norite Tsipringa intrusion, northern Karelia: Geologic structure and petrology. *Petrology* **3**, 645–668.

Sinha A. K. (1969) Removal of radiogenic lead from potassium feldspars by volatilization. *Earth Planet. Sci. Lett.* **7**, 109–115.

Sergeev S. A. et al. (1990) Isotope geochronology of the Vodlozero gneiss complex. *Geochem. Intl.* **27**, 65–74.

Stacey J. S. and Kramers J. D. (1975) Approximation of terrestrial lead evolution by a two-stage model. *Earth Planet. Sci. Lett.* **26**, 207–221.

Tatsumoto M., Knight R. J., and Allègre C. J. (1973) Time differences in the formation of meteorites as determined by $^{207}Pb/^{206}Pb$. *Science* **180**, 1279–1283.

Taylor S. R. and McLennan S. M. (1985) *The Continental Crust, Its Composition, and Evolution.* Blackwell.

Tera F. (1981) Aspects of isochronism in lead isotopic systematics-application to planetary evolution. *Geochim. Cosmochim. Acta* **45**, 1439–1448.

Todt W., Cliff R.A., Hanser A., and Hofmann A.W. (1993) Recalibration of NBS lead standards using a ^{202}Pb-^{205}Pb double spike. *7th Mtg. Eur. Union Geosci. Abst.*, 396 (abstr.).

Turchenko S. I. (1992) Precambrian metallogeny related to tectonics in the eastern part of the Baltic Shield. *Precamb. Res.* **58**, 121–141.

Turchenko S. I. et al. (1991) The Early Proterozoic riftogenic belt of Northern Karelia and associated Cu-Ni, PGE, and Cu-Au mineralizations. *Geol. Fören. I Stockholm Förhandl.* **113**, 70–72.

Vervoort J. D., White W. M., and Thorpe R. I. (1994) Neodymium and lead isotope ratios of the Abitibi greenstone belt: New evidence for very early differentiation of the Earth. *Earth Planet. Sci. Lett.* **128**, 215–229.

Vidal Ph., Blais S., Jahn B. M., and Capdevila R. (1980) U-Pb and Rb-Sr systematics of the Suomussalmi Archean greenstone belt (Eastern Finland). *Geochim. Cosmochim. Acta* **44**, 2033–2044.

Waters F. G., Cohen A. S., O'Nions R. K., and O'Hara M. J. (1990) Development of Archean lithosphere deduced from chronology and isotope chemistry of Scourie dikes. *Earth Planet. Sci. Lett.* **97**, 241–255.

Wooden J. L., Czamanske G. K., and Zientek M. L. (1991) A lead isotopic study of the Stillwater complex, Montana: Constraints on crustal contamination and source regions. *Contrib. Mineral. Petrol.* **107**, 80–93.

You C.-F., Castillo P. R., Gieskes J. M., Chan L. H., and Spivack A. J. (1996) Trace element behavior in hydrothermal experiments: Implications for the fluid processes at shallow depths in subduction zones. *Earth Planet. Sci. Lett.* **140**, 41–52.

Zartman R. E. and Haines S. M. (1988) The plumbotectonic model for lead isotopic systematics among major terrestrial reservoirs - A case for bidirectional transport. *Geochim. Cosmochim. Acta* **52**, 1327–1339.